Some aspects of the analysis of stick-slip vibrations with an application to drill strings

→Proceedings of the 1997 ASME Design Engineering Technical Conferences, Sept 14-17, 1997, Sacramento (CD-rom)

Some Aspects of the Analysis of Stick—Slip Vibrations with an Application to Drill Strings

B. L. van de Vrande D. H. van Campen A. de Kraker

Department of Mechanical Engineering, Eindhoven University of Technology,
P. O. Box 513, 5600 MB Eindhoven, The Netherlands

Abstract—This paper deals with a systematic procedure to calculate periodic solutions of dynamic systems experiencing dry friction. In this first attempt we limit ourselves to 1 and 2 dof autonomous models where a smooth approximation of the discontinuous friction force is applied to avoid numerical difficulties. Using the simple shooting method with a numerical integration scheme suitable for stiff differential equations in combination with a path following algorithm, branches of periodic solutions can be followed for a varying design variable. This approach proves to work very well and will be the basis for developing a numerical tool to investigate more complex mdof dynamic systems with stick—slip phenomena.

1 Introduction

In engineering practice, dry friction often causes undesirable side effects. It can induce a self-sustained stick—slip vibration that can produce noise and may shorten the lifespan of mechanical parts. Examples of such a vibration can be observed in grating brakes and chattering machine tools. Some stick—slip vibrations experienced in everyday life are squeaking chalks and creaking doors.

The general model to describe a dry friction force is given by

$$\begin{cases} |F| \leq \mu_0 F_{\mathrm{N}} & \text{if } v_{\mathrm{rel}} = 0 \\ F = -\mu F_{\mathrm{N}} \operatorname{sgn} v_{\mathrm{rel}} & \text{if } v_{\mathrm{rel}} \neq 0 \end{cases} \tag{1}$$

in which F is the friction force, F_{N} the normal force, v_{rel} the relative velocity, μ_0 the constant static friction coefficient and μ the dynamic friction coefficient which is a function of $|v_{\mathrm{rel}}|$. In literature the dependence of the dynamic friction coefficient on the relative velocity is modeled in different ways. In Coulomb's friction law, μ is assumed to be constant with $\mu \leq \mu_0$. In most other models, μ is modeled as a decreasing function of $|v_{\mathrm{rel}}|$. This decrease has also been observed in experiments (see Popp and Stelter [8]).

The motivation for this work is the torsional stick—slip vibration that occurs in oil exploration drill strings, mainly consisting of a slender steel tube called drill pipe. At the lower part of the drill string, drill collars (thick walled pipes) and stabilizers (cylindrical elements that fit loosely in the bore hole) are used to avoid buckling. At the top, the drill string is supported by a drilling rig. Between the drill bit, the drill collars and the stabilizers on the one hand and the soil on the other hand dry friction occurs, causing the observed stick—slip vibration. During this vibration, the rotational speed at the top of the drill string is approximately constant, whereas the speed at the bit varies between zero (the stick phase) and a speed that is several times higher than the average speed at the top (during the slip phase).

Because of the discontinuity in the friction force, highly nonlinear differential equations arise when dynamic systems experiencing dry friction are modeled. The objective of this work is to find systematically periodic solutions of autonomous stick—slip models using module STRDYN of the finite element code DIANA [1], applying a smooth approximation of the friction force. Module STRDYN comprises several numerical algorithms to investigate finite element models with local

nonlinearities. The simple shooting method (see Parker and Chua [7] or Van de Vorst [9]) is used to determine periodic solutions along with a path following algorithm (see Fey [2]) to calculate branches of periodic solutions if a design variable of the system is changed.

2 Models with Dry Friction

2.1 1 Dof Model

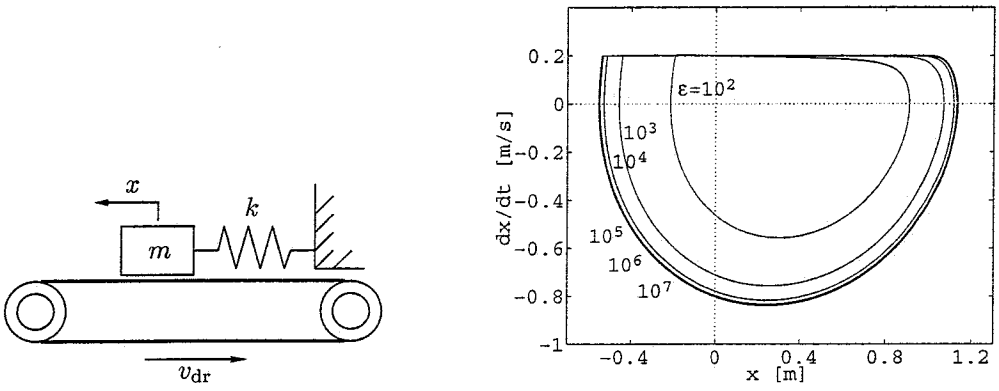

Figure 1: (a) 1 dof model with dry friction, (b) periodic solution at $v_{\mathrm{dr}} = 0.2$ [m/s]

A 1 dof model with dry friction (taken from Galvanetto *et al.* [3]) is depicted in Fig. 1(a). The mass $m = 1$ [kg] is attached to inertial space by the spring $k = 1$ [N/m]. The mass is riding on a driving belt that is moving at the constant velocity v_{dr}. Between the mass and the belt dry friction occurs. The equation of motion of this model reads

$$m\ddot{x} + kx = F \tag{2}$$

in which a dot ($\dot{}$) denotes a differentiation to time t and F is the friction force acting on the mass given by (1). $F_{\mathrm{s}} = \mu_0 F_{\mathrm{N}} = 1$ [N] is the maximum static friction force and $v_{\mathrm{rel}} = \dot{x} - v_{\mathrm{dr}}$ is the relative velocity of the mass with respect to the belt. The dynamic friction coefficient is given by $\mu = \mu_0/(1 + \delta|v_{\mathrm{rel}}|)$, where the positive parameter $\delta = 3$ [s/m] measures the rate at which μ decreases with an increase in $|v_{\mathrm{rel}}|$. The friction force is approximated by the smooth function

$$-2\mu F_{\mathrm{N}} \arctan(\varepsilon v_{\mathrm{rel}})/\pi \tag{3}$$

A large value of ε gives a good approximation but causes a steep slope at $v_{\mathrm{rel}} = 0$ given by $-2\varepsilon F_{\mathrm{s}}/\pi$. This makes (2) stiff so the backward difference method (see Hindmarsh [5]) is used for numerical integration in the shooting procedure.

In Fig. 1(b) the stable periodic solution at $v_{\mathrm{dr}} = 0.2$ [m/s] is shown for $\varepsilon = 10^i$, $i = 2, \ldots, 7$. To investigate the accuracy of the approximation a semi-analytic solution is calculated by applying Hénon's [4] method to integrate over the discontinuity with a 4th-order Runge–Kutta scheme. This solution coincides with the solutions for $\varepsilon \geq 10^5$ in Fig. 1(b). Using the semi-analytic solution, the relative errors e_x in the absolute maximum of x and e_f in the free frequency of the approximations are determined. Table 1(a) shows these errors as a function of ε. Least squares fits with the function $e = b\varepsilon^a$ give $a = -0.59$, $b = 3.3$ for e_x and $a = -0.60$, $b = 3.9$ for e_f. The evolution of the parameters a and b as a function of v_{dr} is given in table 1(b). It can be seen that a is approximately constant and b increases when the velocity of the belt is decreased. Also a is about equal for both e_x and e_f, whereas b is larger for e_f than for e_x. Therefore, the choice of parameter ε should be based on the error in the free frequency at the lowest value of v_{dr} that is of interest.

ε	10^2	10^3	10^4
e_x	0.20	0.059	0.016
e_f	0.24	0.062	0.016
ε	10^5	10^6	10^7
e_x	0.0040	0.00097	0.00023
e_f	0.0041	0.00099	0.00023

	v_{dr}	0.05	0.1	0.15	0.2
e_x	a	-0.58	-0.57	-0.57	-0.59
	b	4.7	3.5	3.2	3.3
e_f	a	-0.60	-0.61	-0.61	-0.60
	b	11	8.1	5.6	3.9

Table 1: (a) Errors e_x and e_f at $v_{\mathrm{dr}} = 0.2$ [m/s], (b) Parameters a and b

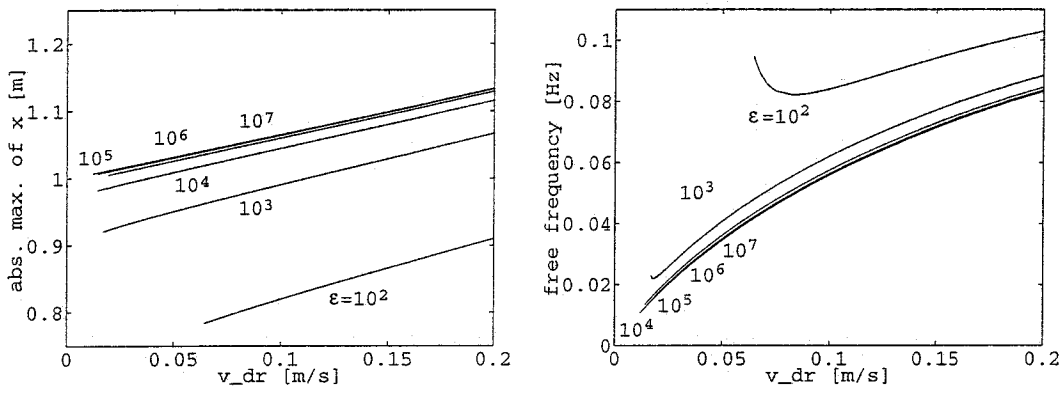

Figure 2: (a) Absolute maximum of x, (b) free frequency

The velocity of the driving belt is used as the design variable and is decreased from 0.2 [m/s] towards 0. Figs. 2(a) and (b) show the absolute maximum of x and the free frequency of the periodic solutions as a function of v_{dr} for $\varepsilon = 10^i$, $i = 2, \ldots, 7$. The branches do not reach $v_{\mathrm{dr}} = 0$, because the step size becomes smaller than the user defined minimum.

If $v_{\mathrm{dr}} \downarrow 0$ the absolute maximum of x should go to 1, because the stick phase ends at $x = F_{\mathrm{s}}/k = 1$ when the elastic force of the spring equals the maximum static friction force. The free frequency should go to 0, because of a longer stick phase at lower driving belt velocities. Clearly, a larger value of ε gives a better correspondence to these conditions. It is also noted that for all values of ε at some point the limit cycle vanishes. This does not correspond to the exact system where a limit cycle exists for all values of $v_{\mathrm{dr}} \neq 0$. The eigenfrequency of the linear system without dry friction is equal to $\sqrt{k/m}/2\pi \approx 0.16$. It is verified that this value is approached by the free frequency if $v_{\mathrm{dr}} \to \infty$.

2.2 2 Dof Model

A 2 dof model with dry friction (also taken from Galvanetto *et al.* [3]) is shown in Fig. 3. The two masses m_1 and m_2 are riding on a driving belt that is moving at the constant velocity v_{dr}. The masses are connected by the spring k_{c} and attached to inertial space by the springs k_1 and k_2. Between the masses and the belt dry friction occurs with friction forces F_1 and F_2 acting on m_1 and m_2, respectively. It is assumed that $m_1 = m_2 = m$ and $k_1 = k_2 = k$. The nondimensional equations of motion are given by

$$\begin{cases} X_1'' + X_1 + \alpha(X_1 - X_2) = F_1^* \\ X_2'' + X_2 + \alpha(X_2 - X_1) = F_2^* \end{cases} \tag{4}$$

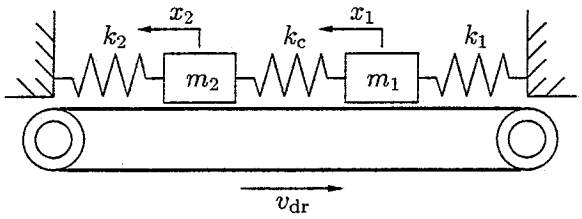

Figure 3: 2 dof model with dry friction

in which a prime ($'$) denotes a differentiation to $\tau = t\sqrt{k/m}$ (t is time), $X_i = x_i k/F_{s1}$ and $\alpha = k_c/k$. F_1^* and F_2^* are given by

$$\begin{cases} |F_1^*| \le 1 & \text{if } V_{rel,1} = 0 \\ F_1^* = -\operatorname{sgn} V_{rel,1}/(1+\gamma|V_{rel,1}|) & \text{if } V_{rel,1} \neq 0 \end{cases} \tag{5}$$

$$\begin{cases} |F_2^*| \le \beta & \text{if } V_{rel,2} = 0 \\ F_2^* = -\beta \operatorname{sgn} V_{rel,2}/(1+\gamma|V_{rel,2}|) & \text{if } V_{rel,2} \neq 0 \end{cases} \tag{6}$$

where $V_{rel,i} = X_i' - V_{dr}$, $V_{dr} = (\sqrt{km}\, v_{dr})/F_{s1}$ and $\beta = F_{s2}/F_{s1}$. F_{si} is the maximum static friction force on mass m_i. The following values are chosen.

$$\alpha = 1.2, \quad \beta = 1.3, \quad \gamma = 3 \tag{7}$$

F_1^* and F_2^* are approximated, respectively, by the smooth functions

$$-2\arctan(\varepsilon V_{rel,1})/\pi(1+\gamma|V_{rel,1}|) \quad \text{and} \quad -2\beta\arctan(\varepsilon V_{rel,2})/\pi(1+\gamma|V_{rel,2}|) \tag{8}$$

According to table 1(b) a minimal accuracy of about 1 % is obtained for $V_{dr} > 0.05$ if $\varepsilon = 10^5$ is chosen. Simple shooting with backward difference integration is used to determine periodic solutions.

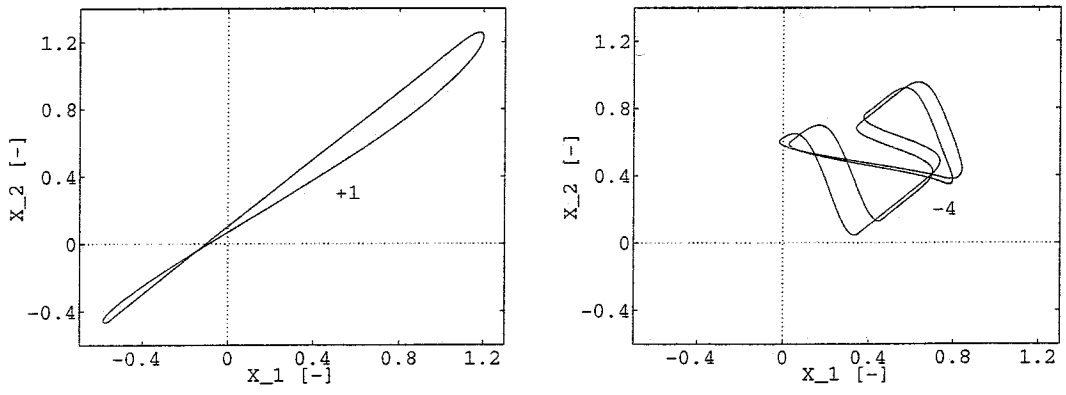

Figure 4: Stable (a) 'in phase' and (b) 'out of phase' periodic solution at $V_{dr} = 0.14$

Fig. 4 shows two stable solutions at $V_{dr} = 0.14$, where X_2 is plotted against X_1. Fig. 4(a) represents an 'in phase' period–1 solution, where 'in phase' means that the two masses are roughly moving in the same direction. A period–n solution is defined as a periodic solution that crosses the Poincaré section defined by $X_1' = 0$, n times from a negative to a positive value during its minimum period. Fig. 4(b) shows an 'out of phase' period–4 solution where the two masses are roughly moving in opposite directions.

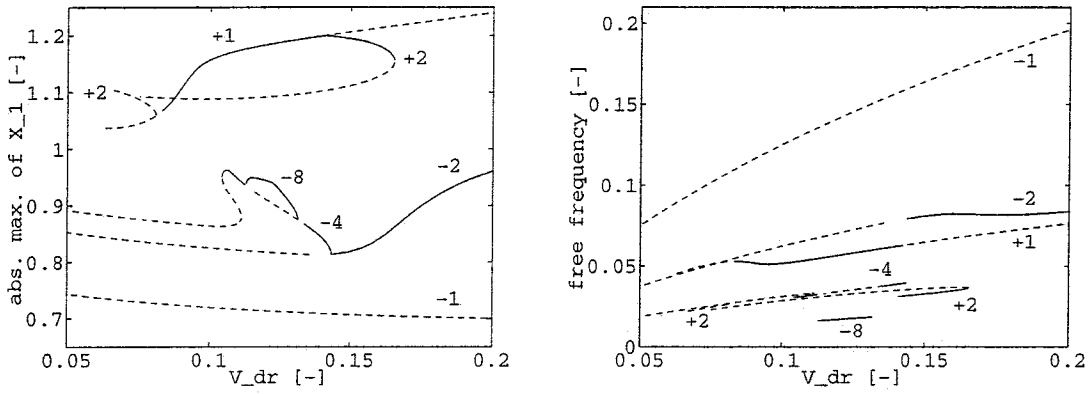

Figure 5: (a) Absolute maximum of X_1, (b) free frequency

Path following is performed with V_{dr} as the design variable. Figs. 5(a) and (b) show the absolute maximum of X_1 and the free frequency of the periodic solutions, respectively. In these figures solid lines represent stable solutions and dashed lines unstable ones. Also $+n$ indicates an 'in phase' period–n solution branch, whereas $-n$ means 'out of phase' period–n. Both for low driving belt velocities and higher period solution branches the step size becomes very small, causing long CPU times.

The eigenfrequencies of the linear system without dry friction are given by $1/2\pi \approx 0.16$ and $\sqrt{1+2\alpha}/2\pi \approx 0.29$. It is verified that these frequencies are approached by the free frequencies of the $+1$ and -1 branches, respectively, if $V_{\mathrm{dr}} \to \infty$.

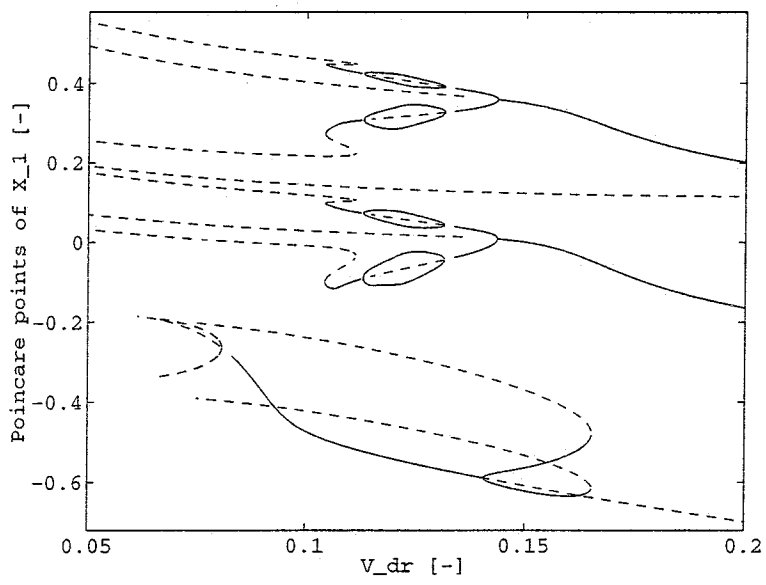

Figure 6: Bifurcation diagram

A bifurcation diagram similar to that given by Galvanetto *et al.* [3] is shown in Fig. 6. In this figure, the Poincaré points of X_1 are plotted against V_{dr}. In the lower half of this diagram, the 'in phase' solution branches are located. The 'out of phase' solutions are the branches in the upper half. This bifurcation diagram corresponds very well to that given by Galvanetto. However, we also found branches with unstable solutions and some extra stable 'out of phase' period–4 solutions at $V_{\mathrm{dr}} \approx 0.111$ not given by Galvanetto.

Several bifurcations can be observed. The 'in phase' period–1 branch shows super-critical flip bifurcations at $V_{dr} = 0.081$ and 0.141. The period–2 branch starting at 0.081 has a flip bifurcation at $V_{dr} = 0.08$. The period–2 branch that is born at 0.141 undergoes a cyclic fold bifurcation at $V_{dr} = 0.165$. At $V_{dr} = 0.144$ a stable period–4 branch originates from the 'out of phase' period–2 branch by a flip. This period–4 branch loses its stability at 0.132 and regains it at 0.113 also by flip bifurcations. Between these bifurcation points, a stable period–8 branch exists. In the period–4 branch, cyclic fold bifurcations occur at $V_{dr} = 0.104$ and 0.1112 and another flip is observed at 0.1106. Between the bifurcation points at $V_{dr} = 0.1112$ and 0.1106 the extra stable 'out of phase' period–4 solutions mentioned before are located.

The CPU time needed to perform the path following calculations for $\varepsilon = 10^5$ is about 9 hours.

3 Drill String Model

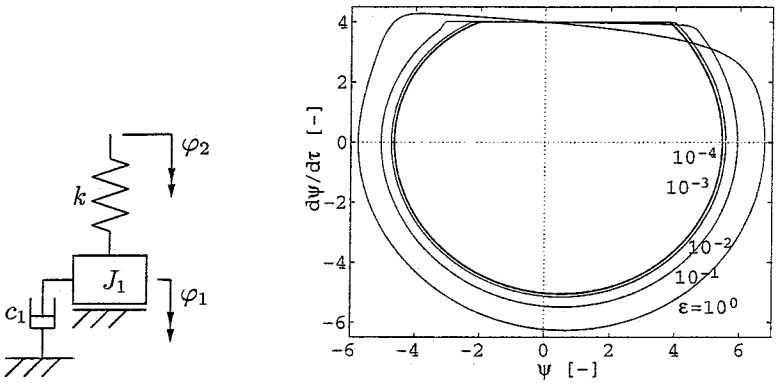

Figure 7: (a) Drill string model, (b) periodic solution at $\eta = 4$

A 1 dof model for investigating the torsional vibration in drill strings is proposed by Jansen [6]. In this model, the drill pipe is modeled by a linear torsional spring k as shown in Fig. 7(a). The drill collars are assumed to be rigid and are modeled as an equivalent mass moment of inertia J_1, also taking into account the mass moment of inertia of the drill pipe. Viscous damping is introduced by the linear torsional damper c_1. The angular displacement of the bit and the drill collars is represented by φ_1 while φ_2 is the angular displacement of the rotary table. Between J_1 and inertial space dry friction occurs. Choosing $\varphi = \varphi_2 - \varphi_1$ as the generalized coordinate and assuming that the rotary table is rotating at the constant speed Ω_2, the equation of motion becomes

$$J_1\ddot{\varphi} + c_1\dot{\varphi} + k\varphi = -T_b + c_1\Omega_2 \tag{9}$$

in which a dot ($\dot{}$) denotes a differentiation to time t and T_b is the friction torque acting on J_1. Coulomb friction is assumed with the maximum static friction torque T_{st} that is larger than the constant dynamic friction torque T_{sl}. If $\Omega_2 > 0$, (9) possesses an equilibrium point at $\varphi = \varphi_{eq} = (T_{sl} + c_1\Omega_2)/k$. To simplify the analysis the following nondimensional quantities are introduced.

$$\tau = \omega t, \quad \psi = \varphi - \varphi_{eq}, \quad \eta = \frac{\Omega_2}{\omega}, \quad \theta = \frac{T_{st} - T_{sl}}{k}, \quad \zeta = \frac{c_1}{2J_1\omega} \tag{10}$$

with $\omega = \sqrt{k/J_1}$ the angular eigenfrequency of the linear system without dry friction. Parameters θ and ζ are chosen equal to 4.2 and 0.05, respectively. Now the nondimensional equation of motion is given by

$$\psi'' + 2\zeta\psi' + \psi = T_b^* \tag{11}$$

ε	10^0	10^{-1}	10^{-2}
e_ψ	0.24	0.090	0.023
e_f	0.077	0.023	0.0053
ε	10^{-3}	10^{-4}	
e_ψ	0.0053	0.0012	
e_f	0.0012	0.00026	

	η	1	2	3	4
e_ψ	a	0.63	0.55	0.54	0.59
	b	0.30	0.25	0.28	0.30
e_f	a	0.63	0.51	0.46	0.62
	b	0.22	0.16	0.093	0.086

Table 2: (a) Errors e_ψ and e_f at $\eta = 4$, (b) Parameters a and b

in which a prime ($'$) denotes a differentiation to τ and $T_b^* = -(T_b + T_{sl})/k$. It is assumed that the drill bit does not rotate backwards and thus $\psi' \leq \eta$. Then T_b^* can be approximated by the smooth function

$$\begin{cases} 0 & \text{if } \psi' \leq \eta - 4\varepsilon \\ -\theta(\psi' - \eta)(\psi' - \eta + 4\varepsilon)^3/27\varepsilon^4 & \text{if } \psi' > \eta - 4\varepsilon \end{cases} \tag{12}$$

Decreasing ε will improve the approximation.

In Fig. 7(b) the stable periodic solution at the nondimensional speed $\eta = 4$ is shown for $\varepsilon = 10^{-i}$, $i = 0, \ldots, 4$, calculated with the simple shooting method using backward difference integration. Because the exact system is piecewise linear, it can be solved semi-analytically. During the stick phase, $\psi' = \eta$. When $\psi = \theta - 2\zeta\eta$ the stick phase ends and the drill string starts to slip. In the slip phase, ψ is given by

$$\psi = e^{-\zeta\tau}\left(\psi_0 \cos\sqrt{1-\zeta^2}\tau + \frac{\psi_0' + \zeta\psi_0}{\sqrt{1-\zeta^2}} \sin\sqrt{1-\zeta^2}\tau\right) \tag{13}$$

in which $\psi_0 = \theta - 2\zeta\eta$ and $\psi_0' = \eta$. The slip phase ends when $\psi' = \eta$. This point can be found with the Newton–Raphson algorithm. The semi-analytic solution coincides with the solutions for $\varepsilon \leq 10^{-3}$ in Fig. 7(b). Using this solution, the relative errors e_ψ in the absolute maximum of ψ and e_f in the free frequency of the approximations are calculated. Table 2(a) shows these errors as a function of ε. Least squares fits with the function $e = b\varepsilon^a$ give $a = 0.59$, $b = 0.30$ for e_ψ and $a = 0.62$, $b = 0.086$ for e_f. The evolution of the parameters a and b as a function of the nondimensional speed η is given in table 2(b).

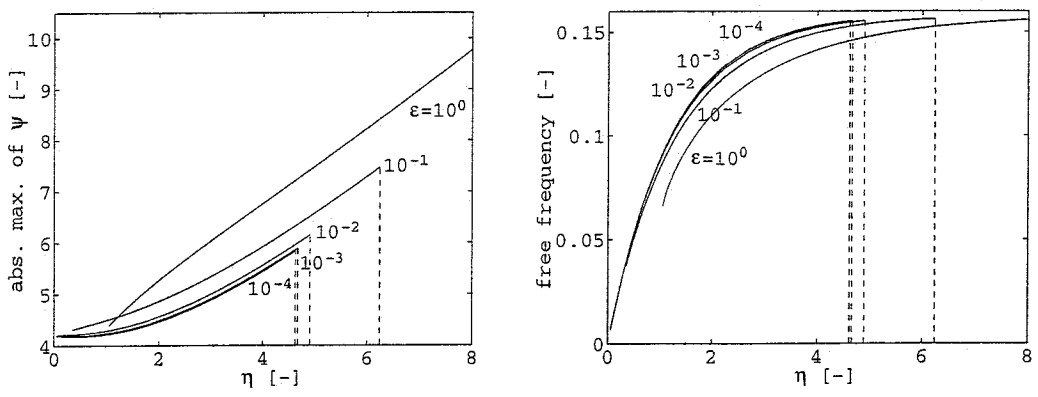

Figure 8: (a) Absolute maximum of ψ, (b) free frequency

This parameter η is used as the design variable in path following and is subsequently decreased from 4 towards 0 and increased from 4. Figs. 8(a) and (b) show the absolute maximum of ψ and the free frequency of the periodic solutions as a function of η for $\varepsilon = 10^{-i}$, $i = 0, \ldots, 4$.

If $\eta \downarrow 0$ the absolute maximum of ψ should approach $\theta = 4.2$, the point at which the stick phase ends. The free frequency should approach 0 because of a longer stick phase at lower values of η. At $\eta \approx 4.61$ the limit cycle should disappear, because of the fact that due to damping, ψ' does not become equal to η anymore and the stable equilibrium point at $\psi = 0$ is reached. Smaller values of ε show a better correspondence to these conditions. It is noted however that also for all values of ε the limit cycle disappears if $\eta \downarrow 0$, which does not correspond to the exact system. The free frequency approaches the expected value of $1/2\pi \approx 0.16$ if $\eta \to \infty$.

4 Conclusions

Using a smooth approximation of the friction force, systems experiencing dry friction can successfully be modeled. By application of the simple shooting method with backward difference integration in combination with the path following algorithm, branches of periodic solutions can be followed for a varying design variable. The approach applied in this paper promises to be a good basis for developing a numerical tool to investigate more complex mdof systems with stick—slip phenomena.

References

[1] DIANA *User's Manual, release 6.0,* TNO Building and Construction Research, Delft, The Netherlands, 1995.

[2] Fey, R. H. B., *Steady-State Behaviour of Reduced Dynamic Systems with Local Nonlinearities,* Ph.D. thesis, Eindhoven University of Technology, Eindhoven, The Netherlands, 1992.

[3] Galvanetto, U., Bishop, S. R. and Briseghella, L., Mechanical Stick—Slip Vibrations, *International Journal of Bifurcation and Chaos,* Vol. 5, No. 3, pp. 637–651, World Scientific Publishing Company, 1995.

[4] Hénon, M., On the Numerical Computation of Poincaré Map, *Physica D* 5, pp. 412–414, 1982.

[5] Hindmarsh, A. C., ODEPACK, A Systematized Collection of ODE Solvers, *Scientific Computing,* Vol 1, Stepleman, R. *et al.* (eds.), pp. 55–64. IMACS/North-Holland Publishing Company, Amsterdam, 1983.

[6] Jansen, J. D., *Nonlinear Dynamics of Oilwell Drillstrings,* Ph.D. thesis, Delft University Press, Delft, The Netherlands, 1993.

[7] Parker, T. S. and Chua, L. O., *Practical Numerical Algorithms for Chaotic Systems,* Springer-Verlag, New York, 1989.

[8] Popp, K. and Stelter, P., Nonlinear Oscillations of Structures Induced by Dry Friction, *Nonlinear Dynamics in Engineering Systems,* IUTAM Symposium Stuttgart/Germany 1989, pp. 233–240, Springer-Verlag, Berlin Heidelberg, 1990.

[9] Van de Vorst, E. L. B., *Long Term Dynamics and Stabilization of Nonlinear Mechanical Systems,* Ph.D. thesis, Eindhoven University of Technology, Eindhoven, The Netherlands, 1996.